SCIENCE CHINA
Earth Sciences

SPECIAL TOPIC: Challenges and uncertainties of ENSO prediction: Enlightenments from El Niño event of 2014–2016
• RESEARCH PAPER •

September 2017 Vol.60 No.9: 1601–1613
doi: 10.1007/s11430-016-0201-9

Processes involved in the second-year warming of the 2015 El Niño event as derived from an intermediate ocean model

ZHANG RongHua[1,2,3*] & GAO Chuan[1,3]

[1] *Key Laboratory of Ocean Circulation and Waves, Institute of Oceanology, Chinese Academy of Sciences, Qingdao 266071, China;*
[2] *Laboratory for Ocean and Climate Dynamics, Qingdao National Laboratory for Marine Science and Technology, Qingdao 266237, China;*
[3] *University of Chinese Academy of Sciences, Beijing 100049, China*

Received October 24, 2016; accepted December 19, 2016; published online January 24, 2017

Abstract The tropical Pacific experienced a sustained warm sea surface condition that started in 2014 and a very strong El Niño event in 2015. One striking feature of this event was the horseshoe-like pattern of positive subsurface thermal anomalies that was sustained in the western-central equatorial Pacific throughout 2014–2015. Observational data and an intermediate ocean model are used to describe the sea surface temperature (SST) evolution during 2014–2015. Emphasis is placed on the processes involved in the 2015 El Niño event and their relationships with SST anomalies, including remote effects associated with the propagation and reflection of oceanic equatorial waves (as indicated in sea level (SL) signals) at the boundaries and local effects of the positive subsurface thermal anomalies. It is demonstrated that the positive subsurface thermal anomaly pattern that was sustained throughout 2014–2015 played an important role in maintaining warm SST anomalies in the equatorial Pacific. Further analyses of the SST budget revealed the dominant processes contributing to SST anomalies during 2014–2015. These analyses provide an improved understanding of the extent to which processes associated with the 2015 El Niño event are consistent with current El Niño and Southern Oscillation theories.

Keywords 2015 El Niño event, Intermediate ocean model, Process analyses, SST budget

Citation: Zhang R H, Gao C. 2017. Processes involved in the second-year warming of the 2015 El Niño event as derived from an intermediate ocean model. Science China Earth Sciences, 60: 1601–1613, doi: 10.1007/s11430-016-0201-9

1. Introduction

The El Niño and Southern Oscillation (ENSO) phenomenon exhibits great diversity and variability, as indicated by observations and model simulations. During 2014–2015, for example, the tropical Pacific experienced a sustained warm sea surface temperature (SST) condition (McPhaden, 2015). There was weak warming in early 2014, a pause in warming in mid-2014, and amplified second-year warming in 2015, with a strong 2015 El Niño event. One notable feature of the 2015 El Niño event was the persistence of a warm SST anomaly throughout 2014–2015 in the western-central tropical Pacific. In particular, the related ocean-atmosphere anomalies were strongly coupled in spring and summer 2015, and these anomalies intensified and developed rapidly into a strong warm event in late spring 2015, reaching a mature El Niño stage late. Note that a similar ocean-atmosphere evolution occurred in early 2014 over the western tropical Pacific, but the warm SST anomalies weakened in mid-2014 and did not sustain and develop into a strong El Niño event in late 2014 (producing only a weak warm condition in 2014; Hu and Fedorov, 2016). It is also worth noting that it had been approximately 5–6 years since the previous El Niño event, which occurred in 2009, representing a long interval between these two El Niño events.

*Corresponding author (email: rzhang@qdio.ac.cn)

In terms of real-time predictions, some coupled models predicted a strong El Niño event in 2014, a false alarm that embarrassed the scientific community. For the 2015 El Niño event, there were large uncertainties regarding its predicted onset using coupled models throughout spring 2015 (Zhang and Gao, 2016b). Additionally, the predicted intensity of the 2015 event ranged widely across coupled models in summer and fall 2015. These differences indicate that real-time predictions of El Niño events remain challenging.

The evolution of the 2015 El Niño event was complex and involved possible interactions with decadal variability and global warming (McPhaden, 2015). Therefore, this event has received considerable attention. The current understanding of the 2015 event is still limited (Hu and Fedorov, 2016; Liu et al., 2015; Min et al., 2015; Zhang and Li, 2015; Zhu et al., 2016; Levine and McPhaden, 2016), including the underlying processes responsible for the persistence of warm SST anomalies throughout 2014–2015, the early onset in March 2015 (rather than in June as in most other events) and the rapid intensification of the ocean-atmosphere anomalies in late spring and summer 2015. Thus, it is important to understand the relevant processes and improve real-time predictions using coupled models.

Previously, we developed an improved intermediate coupled model (ICM) at the Institute of Oceanology, Chinese Academy of Sciences (IOCAS), named the IOCAS ICM (Zhang and Gao, 2016b). One unique feature of the IOCAS ICM is the way in which the temperature of the subsurface water entrained in the mixed layer (T_e) is parameterized: the thermocline effect on SST in the ICM is explicitly represented by the relationship between T_e and sea level (SL; an indicator of thermocline fluctuation). The model has been routinely used to predict SST evolution in the tropical Pacific (for a summary of the model ENSO forecasts, see the International Research Institute for Climate and Society (IRI) website (http://iri.columbia.edu/climate/ENSO/currentinfo/update.html)). When it is forced by prescribed surface wind data, the oceanic component of the IOCAS ICM can accurately simulate the SST evolution during the 2015 El Niño event. In this article, the ocean-only simulation is used to describe the evolution of the 2015 El Niño event. Some specific questions to be addressed include the following: How was the warm SST anomaly sustained in the central equatorial Pacific throughout 2014–2015? What roles did the reflections of oceanic waves (as indicated in the SL signals) at the western and/or eastern boundaries play during 2014–2015? What roles did the subsurface thermal anomalies (as indicated by the T_e fields) play in sustaining the warm SST anomalies during 2014–2015? What processes were involved in the weakening of the warm SST anomalies in 2014 so that conditions in 2014 did not evolve into a strong El Niño event? Is the evolution of the 2015 El Niño event consistent with the processes indicated in the delayed oscillator mechanism?

2. Observational data and the intermediate ocean model

Various observed and reanalysis data are used to describe the evolution of anomalous conditions in the tropical Pacific and to validate model simulations. The SST fields are from Reynolds and Smith (1994), and the wind stress data are from the NCEP/NCAR reanalysis (Kalnay et al., 1996). Oceanic temperature and salinity data are from the gridded Argo products provided by the International Pacific Research Center (IPRC)/Asia-Pacific Data-Research Center (APDRC), which include monthly and long-term climatological mean fields. The monthly mixed layer depth (MLD) and T_e data are also available from the IPRC/APDRC Argo products. The gridded sea level anomalies are from the Ssalto/Duacs multimission altimeter products distributed by Aviso with support from Cnes, which are available online at (http://www.aviso.oceanobs.com/duacs/). Additionally, the real-time evolution of the tropical Pacific ocean-atmosphere anomalies can be seen in the tropical atmosphere ocean (TAO) real-time data, which are available online at (http://www.pmel.noaa.gov/tao/).

The ocean component of an ICM is adopted to depict SST evolution (Zhang et al., 2003, 2005; Zhang and Gao, 2016a). The oceanic dynamic component is an intermediate-complexity model developed by Keenlyside and Kleeman (2002) based on the previous baroclinic modal decomposition approach in the vertical direction (McCreary, 1981). Unlike the commonly used Zebiak-Cane model (Zebiak and Cane, 1987), this relatively newly developed ICM takes into account the spatially varying stratification and the realistic vertical structure of the upper ocean (e.g., ten vertical modes are included). In addition, nonlinear effects in the momentum equation are partially considered so that the zonal currents in the equatorial oceans can be more realistically modeled.

Another crucial component of the ICM is the way in which the subsurface entrainment temperature in the surface mixed layer (T_e) is explicitly parameterized in terms of the thermocline variability (as represented by the SL). An optimized procedure is developed to depict T_e using inverse modeling based on an SST anomaly equation and its empirical relationship with SL variability (Zhang et al., 2005). The model has been successfully used for ENSO simulations and predictions. After optimizing the model performance in terms of ENSO simulations and retrospective ENSO predictions (Zhang and Gao, 2016a), this model was used at the Institute of Oceanology, Chinese Academy of Sciences (IOCAS), and named the IOCAS ICM. Since August 2015, the IOCAS ICM has been routinely used to predict the SST evolution in the tropical Pacific (Zhang and Gao, 2016b). For more information, see the IRI ENSO real-time prediction website.

A statistical wind stress model was constructed using a singular value decomposition (SVD) analysis technique in the tropical Pacific (Zhang et al., 2003). The ocean model simulation forced by the reconstructed wind stress anomalies can realistically depict the spatial structure and time evolution of interannual SST variability. We present process-oriented analyses based on the forced model simulation below.

3. Characteristics of the anomaly evolution during 2014–2015

Figure 1 displays an example for interannual anomalies of SST observed and zonal wind stress obtained from the NCEP/NCAR reanalysis product. The equatorial Pacific experienced sustained warm conditions during 2014–2015, with a dip in the SST in mid-2014 and a rapid warming in May 2015 (Figure 1a); this is accompanied with westerly wind anomalies in the western-central equatorial Pacific (Figure 1b). In the subsurface ocean, positive thermal anomalies persisted in the western-central equatorial Pacific during 2014–2015. For example, SL anomaly signals originating from the western boundary regions are seen to propagate eastward along the Equator and appear to have warming or cooling effects on SSTs in the central and eastern equatorial Pacific. In late 2013, for instance, a positive SL anomaly in the west was observed to propagate eastward along the Equator. Its arrival to the east produced a warming effect in the SSTs during spring 2014. In early 2014, a low SL signal propagated eastward along the Equator to the eastern equatorial Pacific, and its arrival to the east produced a cooling effect on the SSTs in mid-2014. This process is attributed to the weakening of the warm SST anomaly in summer 2014. In spring 2015, SL anomalies intensified in the central equatorial Pacific, but no propagating signals were observed from the western Pacific at this time. Rather, a positive SL anomaly, which formed over the eastern equatorial Pacific in

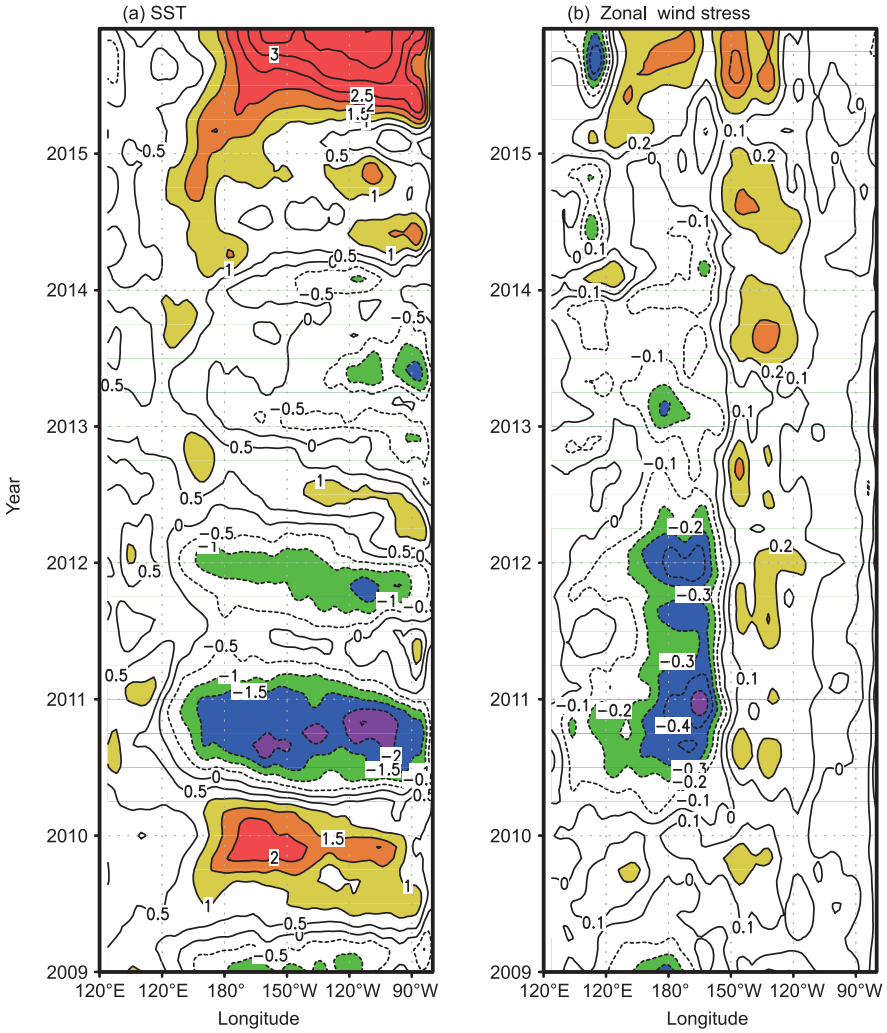

Figure 1 Zonal-time sections of interannual anomalies along the Equator for (a) SST observed and (b) zonal wind stress obtained from the NCEP/NCAR reanalysis product. Linear trend in wind stress anomalies during the period 1980–2015 is removed when they are used to force the ocean model. The contour interval is 0.5°C for SST and 0.1 dyn cm^{-2} for zonal wind stress.

late 2014, reflected off the eastern boundary and propagated westward off the Equator. The penetration of this anomaly into the equatorial region in early 2015 enhanced subsurface thermal anomalies in the central equatorial Pacific. These processes produced large warm SST anomalies in the central-eastern equatorial Pacific, which were accompanied by westerly wind anomalies in the west. Then, the coupling between these SST and wind anomalies led to rapid amplification of the warm SST anomalies in summer 2015, evolving into a strong El Niño event with a peak in late 2015. These features are clearly evident from the TAO observations, which are used to validate model simulations.

Figures 2 and 3 illustrate zonal-time sections of simulated interannual anomalies along the Equator for SST, zonal wind stress, SL and T_e. Note that the wind stress anomalies are derived from observed SST anomalies using an empirical wind stress model constructed from historical data (Zhang et al., 2003) and that the T_e anomalies are derived from the simulated SL anomalies using an empirical T_e model constructed from historical data (Zhang et al., 2005).

The oceanic component of the IOCAS ICM can accurately depict these interannual variabilities compared with corresponding observations (Figure 1a). For example, the model captured the SST evolution in 2009–2015 extremely well (Figure 2a). A weak El Niño event occurred in 2009, followed by La Niña conditions in 2010, with second-year cooling in 2011 (Zhang et al., 2013). Starting from late 2013, El Niño conditions prevailed in the eastern basin. Warm SST anomalies emerged in early 2014 but weakened in summer 2014. Then, warm conditions intensified in late 2014 and early 2015. In mid-2015, warm SST anomalies developed rapidly through ocean-atmosphere coupling, leading to the

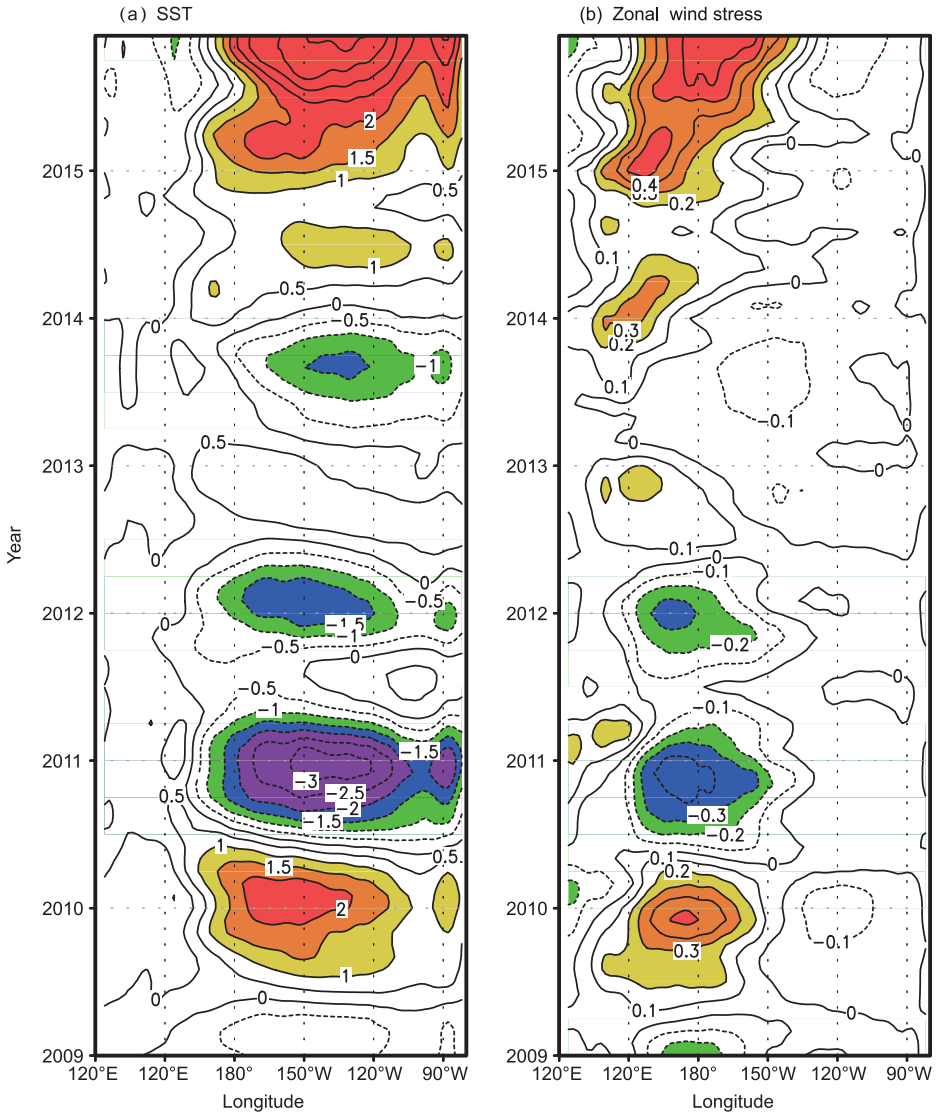

Figure 2 Zonal-time sections of anomalies along the Equator for (a) SST and (b) zonal wind stress. The zonal wind stress anomalies are derived from observed SST anomalies using an empirical wind stress model constructed from historical data of SST and wind stress. The contour interval is 0.5°C for SST and 0.1 dyn cm^{-2} for zonal wind stress.

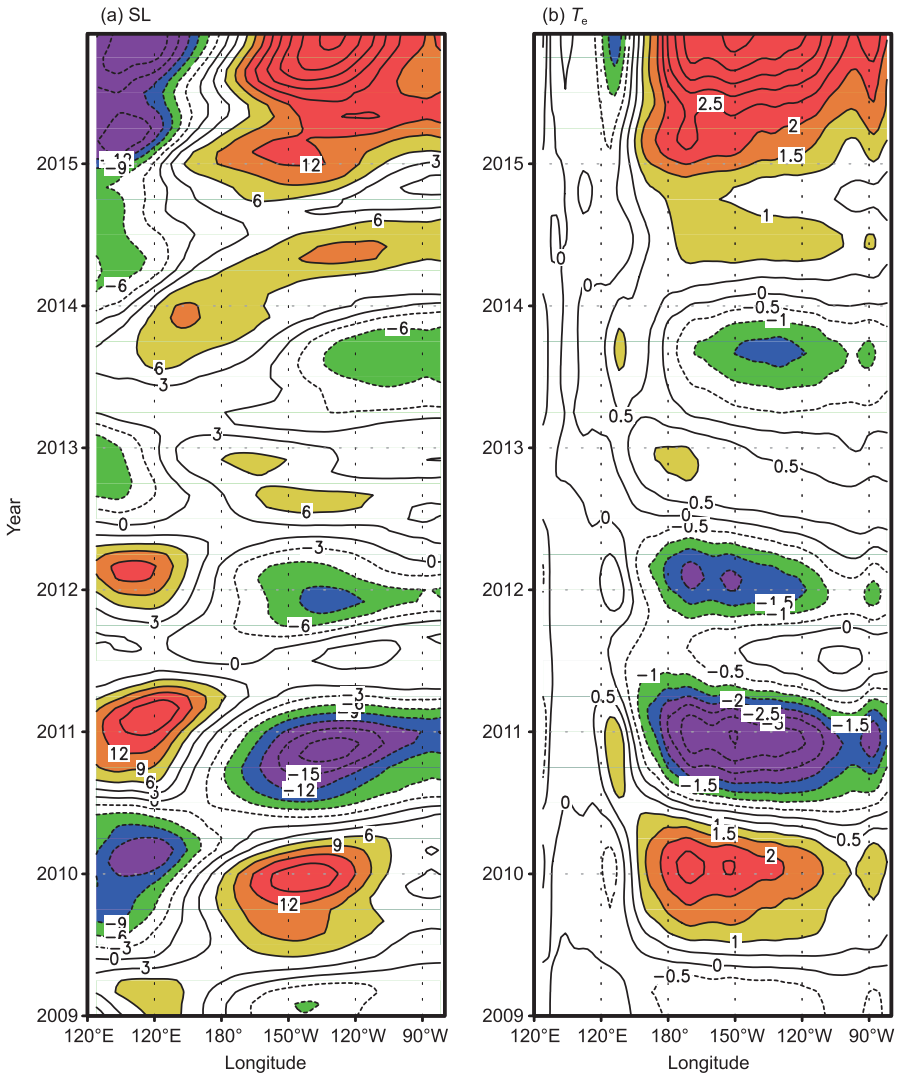

Figure 3 Zonal-time sections of anomalies along the Equator for (a) SL and (b) T_e along the Equator. The T_e anomalies are derived from the simulated SL anomalies using an empirical T_e model constructed from historical data. The contour interval is 3 cm for SL and 0.5°C for T_e.

strong El Niño event in 2015. Note that there was a long interval between the two El Niño events in 2009 and 2015 (approximately 5−6 years).

To illustrate the space-time evolution in more detail, Figures 4 and 5 show the horizontal distributions of some related interannual anomalies simulated using the ocean model during early 2015. Together with Figures 2 and 3, the spatial structure and phase relationships among the anomalies of SST, surface winds, SL and T_e can be more clearly illustrated off and on the Equator. Coherent relationships among these anomalies simulated from the model are used to illustrate relevant processes involved in the 2015 El Niño event. Detailed analyses are given below.

3.1 The persistent warm SST anomalies

One pronounced feature is the persistence of warm SST anomalies during 2014–2015 in the central equatorial Pacific (Figure 2a). For example, warm SST anomalies remained in the equatorial Pacific from the early warm conditions in 2014 and were accompanied by westerly wind anomalies that persisted in the western equatorial Pacific (Figure 2b). A weakening of the warm SST anomalies occurred in mid-2014, accompanied by weakening of the westerly wind anomalies. Warm SST conditions intensified in the eastern equatorial Pacific in late spring 2015 and experienced a rapid amplification of warming in mid-2015, accompanied by westerly wind anomalies (Figure 4).

A key issue is how the warm SST anomaly is sustained in the central equatorial Pacific. Various processes are responsible for these SST anomalies, including remote effects associated with propagating oceanic waves and their reflections at the western and eastern boundaries, local effects associated with positive subsurface thermal anomalies, and wind forcing. These processes collectively acted to determine SST evolution during 2014–2015. The relationships between

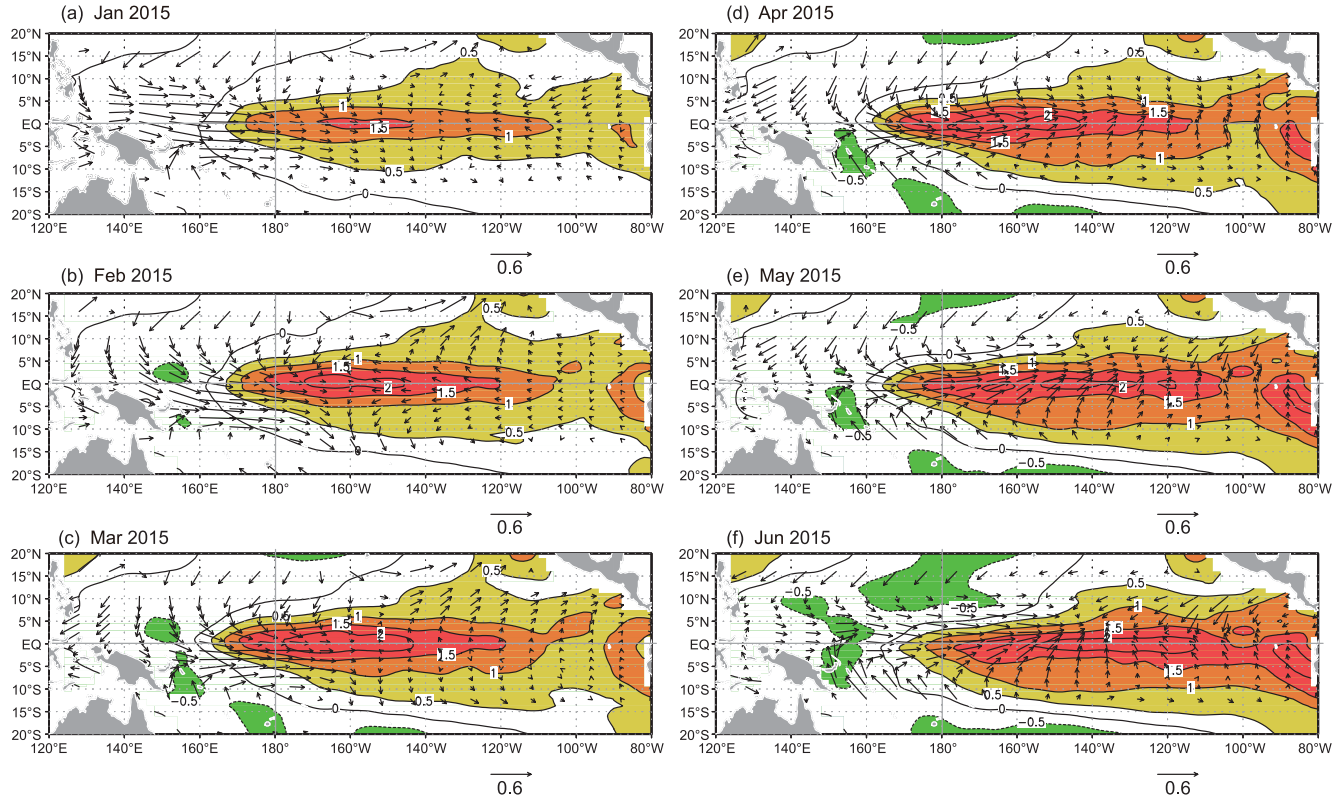

Figure 4 Horizontal distributions of SST anomalies (contours) and surface wind stress (τ) anomalies (vectors): (a) January 2015, (b) February 2015, (c) March 2015, (d) April 2015, (e) May 2015, and (f) June 2015. The contour interval is 0.5°C for SST; the arrow indicates 0.6 dyn cm^{-2} for wind stress.

these processes and the way the SST evolved are analyzed blow.

3.2 Remote effects of propagating oceanic waves and reflections as represented in SL signals

In the ocean, interannual variability in the thermocline exhibits pronounced propagation of equatorial waves, which remotely affect thermal conditions around the basin, thus providing low-frequency memories for the tropical Pacific climate system. For example, SL signals tend to propagate eastward along the Equator and westward off the Equator, and reflect off the western and eastern boundaries (McCreary, 1981; Zebiak and Cane, 1987; Jin and An, 1999; Gao and Zhang, 2017). SST variability in the equatorial Pacific exhibits a coherent relationship with propagating SL signals on and off the Equator and their reflections at the western and eastern boundaries. A few cases can be highlighted during 2014–2015 as follows.

During the La Niña conditions in 2013, for example, there was a buildup of warm waters in the western Pacific Ocean due to stronger-than-normal trade winds in the central basin, with the SL in the west increasing steadily. In late 2013, a positive SL signal was seen to propagate eastward along the Equator from the western boundary (Figure 3a). Its arrival to the east caused a warming effect on the SST in early 2014. Indeed, warm SST conditions emerged to the east (Figure 2a), accompanied by westerly wind anomalies (Figure 2b). In early 2014, an upwelling SL signal originated from the western boundary regions and propagated eastward along the Equator (clearly seen as a propagating low sea level signal; Figure 3a). The arrival of this signal to the east induced a cooling effect on the SST in mid-2014 (Figure 2a). Indeed, the warm SST anomalies in the east weakened in summer 2014 (Figure 2a). This result may explain why SST and wind anomalies did not develop strongly during the summer of 2014. Note that the cooling effect on the SST was not sufficiently strong to reverse the warm SST conditions in the east and thus the warm SST conditions remained in the equatorial Pacific throughout 2014.

In early 2015, SL and SST anomalies intensified in the central equatorial Pacific. At this time, however, no propagating SL signal could be traced to the western boundary regions (Figure 3a). Thus, oceanic processes originating from the western Pacific (i.e., the reflections of SL signals at the western boundary) did not play a major role in the amplification of the warm SST anomalies in the central equatorial Pacific. To explain this phenomenon, processes in the eastern equatorial Pacific must be examined. In late 2014, for example, positive SL anomalies emerged in the eastern equatorial Pacific, which tended to reflect off the eastern boundary and propagate westward off the Equator (e.g., Figure 5a). Strikingly,

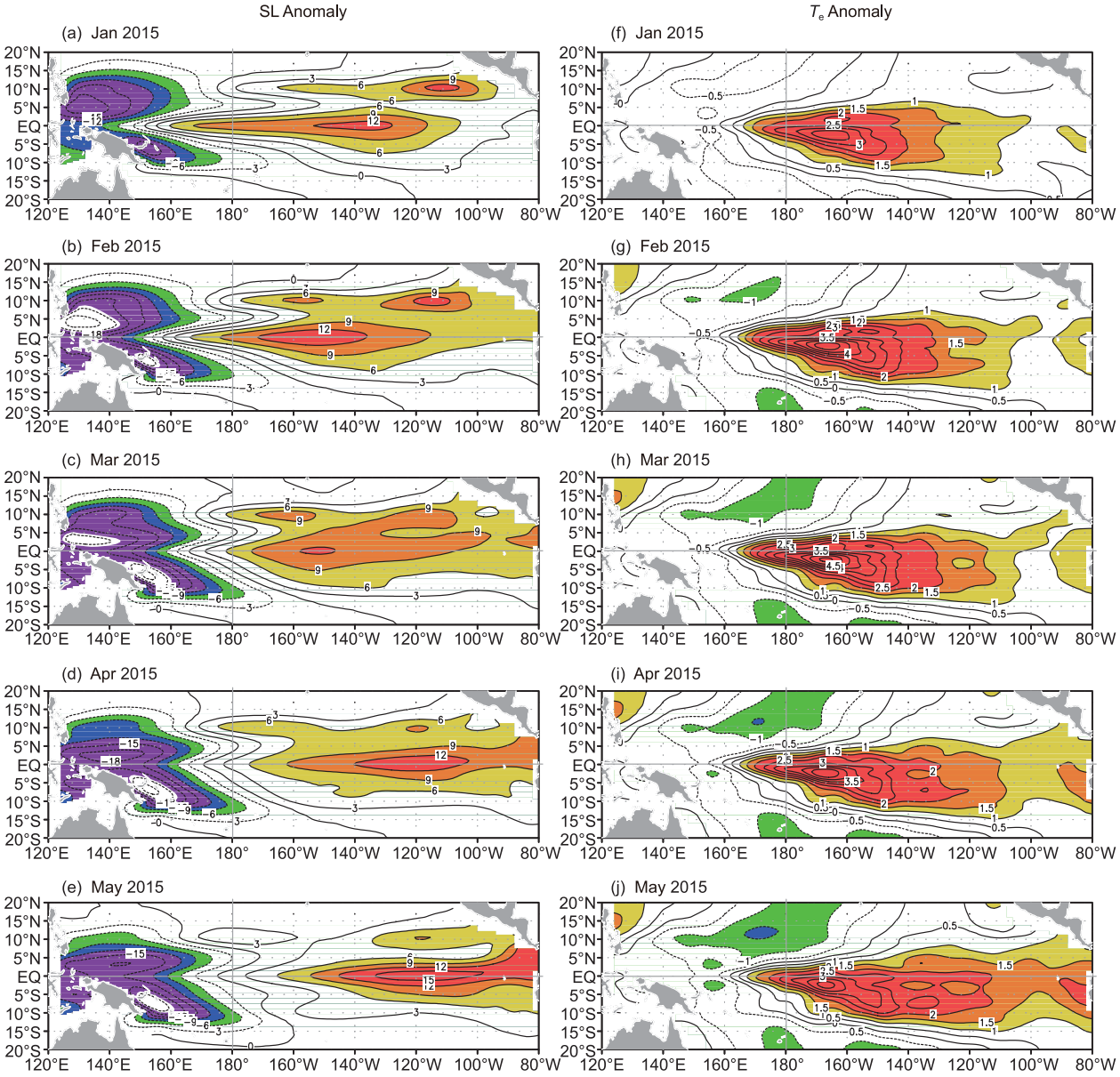

Figure 5 Horizontal distributions of SL (left panels) and T_e (right panels) anomalies simulated using the ocean model for (a), (f) January 2015, (b), (g) February 2015, (c), (h) March 2015, (d), (i) April 2015, and (e), (j) May 2015. The contour interval is 3 cm for SL and 0.5°C for T_e.

these positive SL anomalies penetrated into the central equatorial basin in early 2015 (Figure 5b and c), merging with the positive SL anomalies that persisted in 2014. This process acted to enhance the positive T_e anomalies (Figure 5g–h), thus producing large warming effects on the SST in spring 2015. As such, the reflections of the positive SL anomalies off the eastern boundary and westward propagation off the Equator in the north in late 2014 and early 2015 played an important role in enhancing SST warming in early 2015.

3.3 A subsurface thermal anomaly pattern and its local effects on SST

In addition to the remote effects induced by propagating SL signals, SST variability is determined by local conditions associated with positive subsurface thermal anomalies in the central and eastern equatorial Pacific. In 2014–2015, large positive T_e anomalies persisted in the central equatorial Pacific, characterized by a horseshoe-like pattern connecting subsurface variability off and on the Equator (Figure 5f–j). The importance of this positive T_e pattern in maintaining the warm SST conditions can be illustrated by two examples as follows. One example is associated with the maintenance of the warm conditions in mid-2014. Although an upwelling SL signal propagated eastward along the Equator in early 2014 and its arrival in the east in April-June 2014 had a cooling effect on SST, the warm SST condition prevailed in the eastern equatorial Pacific. Indeed, a weakening of the warm SST

anomalies occurred to the east (Figure 5a). However, the cooling effect associated with the SL propagation from the far western Pacific was not sufficiently strong to fully reverse the warm conditions in the east, and the warm SST conditions remained in the tropical Pacific throughout late 2014. Here, the persistent positive T_e anomalies in the central equatorial Pacific had strong warming effects on SST, acting to sustain the warm SST conditions in mid- and late 2014.

Another example is associated with the development of warm SST anomalies over the central equatorial Pacific in early 2015. At this time, no propagating SL signal could be observed directly from the far western boundary regions. Hence, oceanic processes in the western tropical Pacific (e.g., the reflection of SL signals at the western boundary) did not play a major role in the intensification of warm SST anomalies in the east. By contrast, large positive T_e anomalies persisted and increased in the western-central equatorial Pacific (Figure 5f–j) and played an important role in maintaining warm SST anomalies (Figure 4). In particular, the positive T_e anomalies in the central equatorial region were enhanced by processes in the eastern equatorial Pacific: positive SL anomalies were seen to reflect off the eastern boundary in early 2015, propagate westward off the Equator and penetrate into the equatorial regions, thereby enhancing the positive T_e anomalies in the central basin and producing large warming effects on the SSTs. The induced warm SST anomalies were accompanied by westerly wind anomalies, leading to their coupling. Thus, the persistent positive T_e anomaly pattern during 2014–2015 was a key factor contributing to the sustained warm SST anomaly in the central-eastern equatorial regions.

3.4 The SST budget analyses

An SST budget (the temperature variations within the mixed layer) analysis is performed to determine which physical processes are responsible for the interannual SST variability. The local rate of SST changes (tendency) in the equatorial Pacific is mainly determined by horizontal and vertical advection, vertical and horizontal diffusion, and heat flux at the sea surface. Note that heat flux always has a damping effect on SST anomalies on interannual time scales (Zhang and Gao, 2016a), and it thus is not shown below. Figures 6 and 7 illustrate the spatial distributions of the major SST budget terms for zonal, meridional and vertical advection, vertical diffusion, and their sum in early 2015. The contributions of the different terms to the SST budget varied considerably in space and time, and the relative importance of the individual processes affecting SST variability is clearly illustrated.

As shown above, one pronounced feature was the persistence of a warm SST anomaly in the central equatorial Pacific, with first noticeable warming occurred in May–June 2015 (Figure 2a). Thus, one key question is how this SST warming was sustained. The SST budget analyses indicate that a positive SST tendency appeared near the date line in early 2015 (e.g., Figure 6), which was mainly attributed to the vertical diffusion effect (e. g., Figure 6a4 and Figure 6b4) associated with the positive T_e anomalies (Figure 5f–j). It is thus clear that through vertical diffusion, the positive T_e anomalies induced and sustained the warm SST anomaly near the date line (Figure 4). Additionally, westerly wind anomalies over the western equatorial Pacific directly forced anomalous currents, which induced a warming SST tendency through horizontal advection (e. g., Figure 6a1–a2 and Figure 6b1–b2).

With time, large positive vertical diffusion effects and the associated SST warming appeared to more east, and large warm SST anomalies were present in the eastern equatorial regions that started in May 2015 (Figure 7). On the Equator, for example, the SST budget during the developing stage of El Niño in mid-2015 was dominated by contributions of vertical diffusion and advection in the central and eastern region (Figure 7). In the western Pacific, a negative SST tendency appeared off the equator near the date line in mid-2015 (e.g., Figure 7), which was mainly attributed to the vertical diffusion effect (e. g., Figure 7a4 and Figure 7b4) associated with the negative T_e anomalies (Figure 5f–j).

Thus, supported by a strong T_e influence, SST anomalies were generated and sustained in the equatorial Pacific through vertical diffusion. In particular, the positive T_e anomalies produced SST warming in the equatorial region in early and mid-2015. On the Equator, the positive thermocline effect (associated with the vertical advection of anomalous T_e by the mean upwelling and vertical diffusion) played an important role in the rapid growth of SST anomalies (Jin and An, 1999). These results indicate that T_e plays a dominant role in sustaining warm SST anomalies in the equatorial Pacific. Through the entrainment process, persistent subsurface thermal anomalies can exert direct and immediate influences on the SST over the central and eastern equatorial basin. The results obtained from this work are consistent with previous analyses and modeling studies (Zhang and Gao, 2016a), supporting the dominant role played by subsurface processes in SST evolution in the tropical Pacific.

Based on the analyses above, a schematic diagram presented in Figure 8 shows the processes affecting the SST evolution in 2015. The 2015 El Niño event appeared as a sequence of warm SST conditions that started in 2014, with strong second-year warming occurring in mid- and late 2015, which can be further traced back to the previous year. In 2013, a weak cold SST condition prevailed in the central-eastern tropical Pacific, accompanied by easterly wind anomalies to the west, which induced corresponding consequences in the ocean. Several processes were involved in the subsequent evolution into the second-year warming in 2015. With respect to subsurface anomalies (as represented by SL), propagating SL signals were evident around the basin, remotely influenc-

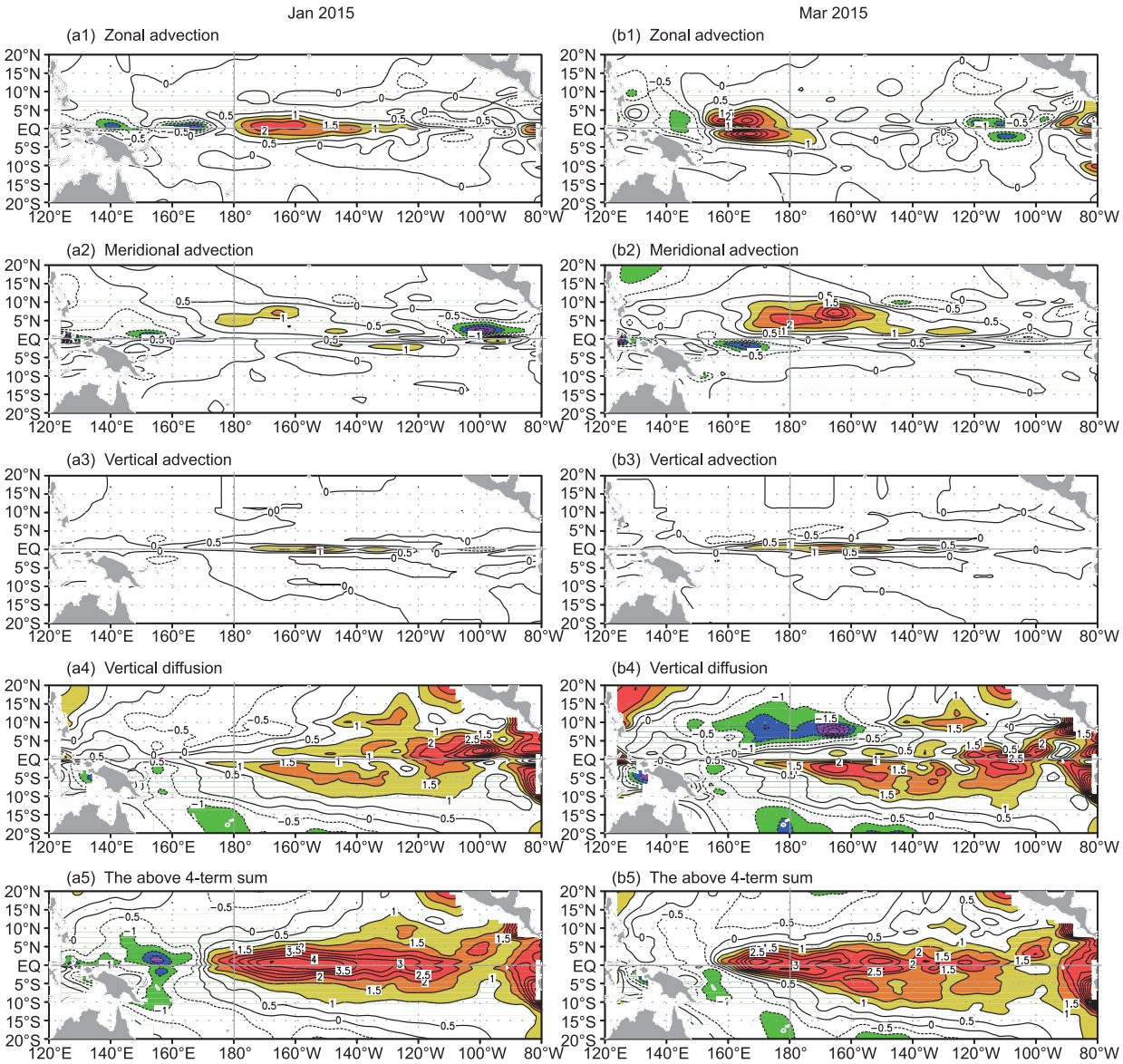

Figure 6 Horizontal distributions of the SST budget terms for zonal advection, meridional advection, vertical advection, vertical diffusion, and the sum of these four terms in January 2015 (left panels) and Mar 2015 (right panels). The contour interval is 0.5°C/month.

ing T_e and SST. Off the Equator, for example, large positive SL anomalies in the east, produced by warm conditions in 2014, propagated westward off the Equator in the north. This off-equatorial positive SL anomaly penetrated into the equatorial regions near the date line in spring 2015, in combination with the positive SL anomalies (Figure 5a–e), enhancing the positive T_e anomalies that persisted(Figure 5f–j). The enhanced positive T_e anomalies in the central-eastern equatorial regions had a large warming effect on SST, producing strong warm SST anomalies, which were accompanied by westerly wind anomalies in the west. In spring 2015, the related anomalies of SST and surface winds intensified through their coupling. A systematic warm SST anomaly was seen in the east in May 2015. By the late spring of 2015, there were notable signs of the developing El Niño conditions at the sea surface.

4. Discussion and conclusion

The tropical Pacific experienced a sustained warm SST condition in 2014–2015, with a strong El Niño event in 2015, which has been a hot topic not only in the scientific community but also among the public and the media. The current understanding of the related SST evolution is still very limited. It is critical to understand the processes involved in the 2015 El Niño event. Previously, we improved the IOCAS ICM, which has been routinely used for real-time ENSO prediction. The oceanic component of the IOCAS ICM forced

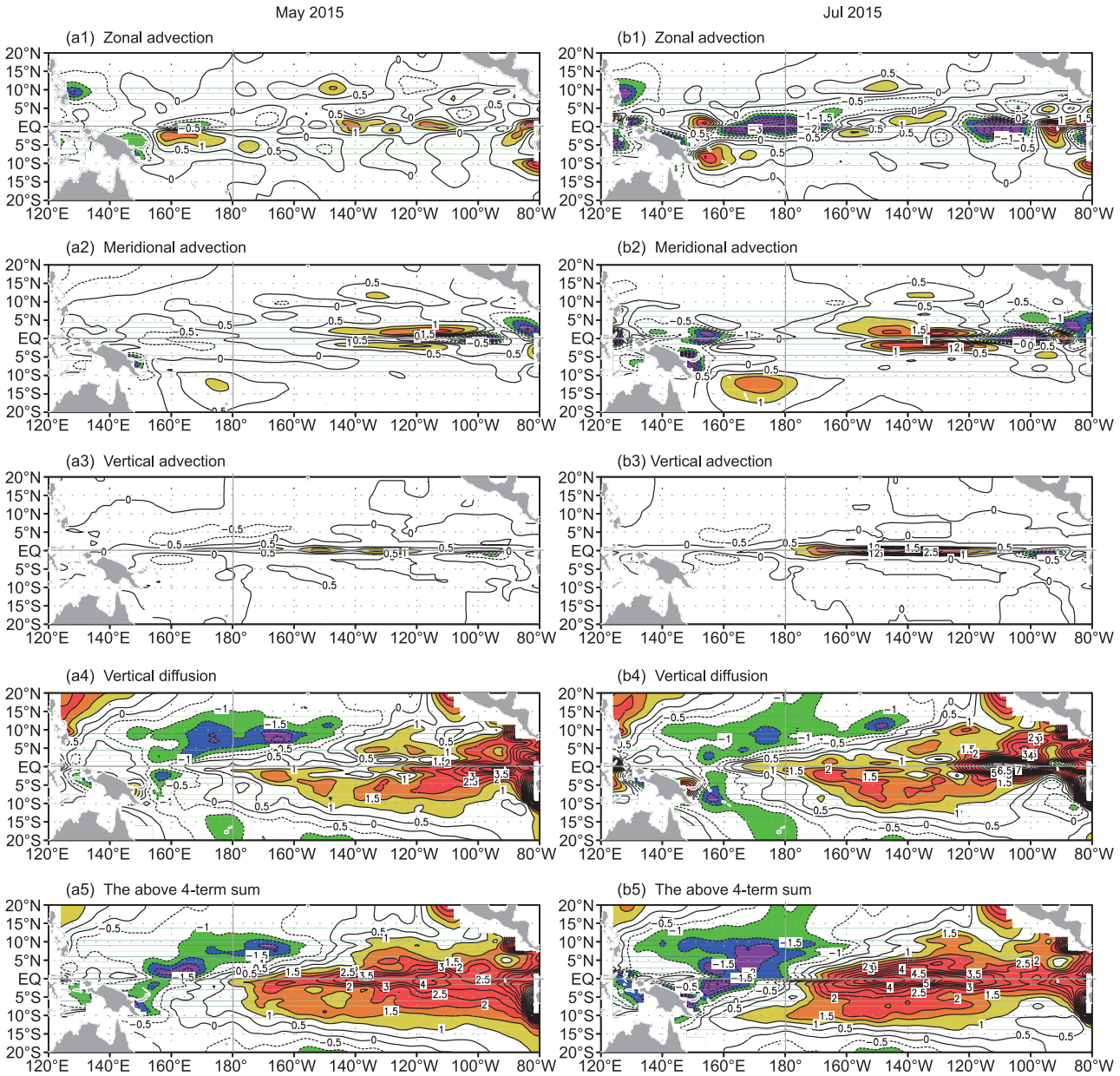

Figure 7 Horizontal distributions of the SST budget terms for zonal advection, meridional advection, vertical advection, vertical diffusion, and the sum of these four terms in May 2015 (left panels) and July 2015 (right panels). The contour interval is 0.5°C/month.

by prescribed surface wind can successfully depict the SST evolution in the equatorial Pacific compared with corresponding observations. In this paper, the oceanic model-based simulations are used to illustrate the relationships between anomaly fields and to reveal the processes important to the 2015 El Niño evolution, with a focus on the extent to which the evolution can be understood in terms of the current ENSO theories.

As indicated by the thermocline feedback (Bjerknes, 1969), large-scale thermocline fluctuations (as indicated in SL signals) and coupling between surface winds and SSTs are important to ENSO cycles. For example, one important process is the large-scale structure of the upper-ocean heat content (as represented by SL) in the tropical Pacific: coherent propagating SL signals around the basin provide low-frequency memory for interannual variability in the system. Indeed, oceanic equatorial wave processes (as indicated by the SL signals) can be clearly traced around the basin. Propagating SL signals and their reflections off the western and/or eastern boundaries induce remote effects on SSTs in the equatorial Pacific, serving as positive and negative feedbacks during ENSO cycles. Additionally, subsurface thermal anomalies produce local effects on SSTs in the central-eastern equatorial Pacific. In particular, large positive subsurface thermal anomalies persisted in the central equatorial Pacific during 2014–2015 and were characterized by a horseshoe-like pattern connecting variability off and on the Equator, thereby sustaining the warm SST

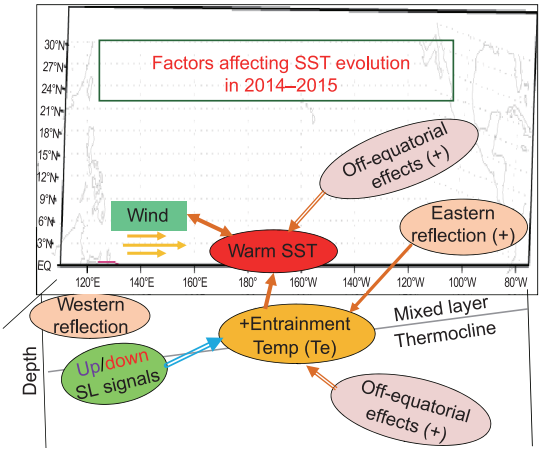

Figure 8 A schematic diagram showing the processes affecting SST conditions during 2015, in which T_e is the temperature of the subsurface water entrained in the mixed layer. In the central equatorial Pacific, large positive T_e anomalies persisted throughout 2014–2015, with a horseshoe-like pattern connecting subsurface thermal variability off and on the Equator. A few processes tended to sustain this T_e pattern. In the atmosphere, westerly wind anomalies were present near and west of the date line during 2015. The wind anomalies suppressed the thermocline, producing positive T_e anomalies in the central domain. In the ocean, positive subsurface thermal anomalies off the Equator were connected to the Equator in the central basin, fostering positive T_e anomalies on the Equator. Additionally, during and after the warm conditions in 2014, positive SL anomalies propagated westward off the Equator from the eastern boundary regions. The penetration of these anomalies into the central equatorial Pacific reinforced the positive T_e anomalies in the central basin.

conditions in the equatorial Pacific. Hence, the combined effects of local processes associated with the persistent positive T_e anomalies and remote processes associated with propagating SL signals collectively determined the SST evolution in the eastern equatorial Pacific. During 2014–2015, for example, positive T_e anomalies prevailed in the central equatorial Pacific, thereby sustaining warm SST conditions in the central-eastern regions. In early 2014, however, a low SL signal propagated eastward on the Equator from the western Pacific, and its arrival to the east in the middle of 2014 weakened the warm SST conditions. Nevertheless, the cooling effect on the SSTs was not sufficiently strong to reverse the warm SST conditions in the east, which were sustained by the positive subsurface thermal anomalies. In this case, the warming effect locally associated with the positive subsurface thermal anomalies in the central-eastern regions counteracted the cooling effect remotely associated with propagating SL signals from the western boundary regions.

In early 2015, large positive SL and SST anomalies emerged in the central equatorial Pacific, but no propagating SL signal can be traced to the western boundary regions at this time. Thus, oceanic processes in the western tropical Pacific (e.g., the reflection of SL signals at the western boundary) did not play a major role in the intensification of the positive SL and SST anomalies. However, large positive T_e anomalies persisted and intensified in the western-central equatorial Pacific, thereby playing an important role in maintaining warm SST anomalies in early 2015. Furthermore, the reflection processes of SL signals were evident in the eastern equatorial Pacific in early 2015: a positive SL signal, which was related to the warm conditions in late 2014, propagated eastward on the Equator into the eastern boundary region, then reflected and propagated westward off the Equator. In early 2015, this positive SL anomaly penetrated into the central equatorial Pacific regions. This process enhanced the positive T_e anomalies in the central equatorial Pacific, producing a large warming effect on SSTs. Note that the penetration of the off-equatorial warm water to the central equatorial region is proposed to be a key process for the 2015 El Niño amplification. As shown in Figure 5b–d, off-equatorial warm signals exhibited westward propagation but cannot reach the western boundary in a coherent way in this year (as the classical theory declares). This is one feature in which the development of the 2015 El Niño event differed from other El Niño events.

This paper focuses on large-scale oceanic processes involved in the evolution of the 2015 El Niño event. Other high-frequency processes may also play important roles and therefore need to be considered in future analyses. As previous studies have indicated, for instance, westerly wind bursts (WWBs) can significantly modulate SST evolution and are responsible for the irregularity in El Niño events (Chen et al., 2015). In particular, strong WWBs were observed over the western Pacific in spring 2015 and may play an important role in the rapid development of the warm SST anomalies. Easterly wind anomalies were also observed to prevail over the central basin in mid-2014 (Hu and Fedorov, 2016; Liu et al., 2015; Min et al., 2015; Zhang and Li, 2015; Levine and McPhaden, 2016) and are considered to play a role in the weakening of the warm SST anomalies. Therefore, wind forcing and its combined effects with oceanic processes need to be taken into account in analyses and modeling.

The effects of other low-frequency processes on the 2015 El Niño evolution also need to be taken into account, including decadal variability and global warming. As indicated above, one important finding from this study is that large off-equatorial positive thermal anomalies from the eastern regions are seen to penetrate into the central equatorial region during the 2015 El Niño, whereas they are not during other previous El Niño events. This can be attributed to a few factors. Besides the dominant interannual variations associated with ENSO, other low-frequency climate variability modes also exist over the Pacific, including the so-called Pacific decadal oscillation (PDO). As observed, the Pacific climate system was in a warm PDO phase during 2000–2014 (but a cold phase during 1980–1999), characterized by a cold SST condition over the tropical Pacific but a warm SST condition in the North Pacific midlatitude regions. There is an indication that this see-saw

pattern of the SST anomalies is likely to change in 2015 after its decade-long persistence. That is, the cold SST condition, which prevailed during 2000–2014, tended to shift to a warm one; this PDO phase transition likely led to change in the mean climate state over the Pacific in 2015. In addition, a global warming signature is also evident over the region: the mean SST field in the tropical Pacific turned to a warming trend after a decade-long cooling tendency over the early period of this century (the so-called hiatus of global warming). Also, large positive thermal anomalies were seen to merge in the northeastern tropical Pacific, with warm signals penetrating into the central equatorial Pacific. Obviously, the 2015 El Niño evolution was modulated by the decadal change and global warming effects, leading to a decade change in the mean ocean thermal condition over the Pacific.

Climatologically, subsurface thermal field (as indicated in sea level) exhibits well-defined trough and ridge structures in the tropical Pacific, with a ridge along 10°N and a trough on the equator. From dynamical point of view, a related potential vorticity (PV) pattern is seen in the tropical-subtropical Pacific, characterized by a local minimum in the eastern tropical Pacific off the equator; this PV pattern tends to prevent off-equatorial waters from penetrating into the equator. When there are changes in the mean oceanic thermal state in the tropical Pacific (e.g., a spatial shift in the mean thermal trough-ridge pattern), the amplitude and structure of the local mean PV field in the eastern tropical Pacific can be modulated, leading to possible changes in the propagation pathways of thermal anomalies in the tropical Pacific. Preliminary analyses indicate that the changes in the mean thermal condition and PV field over the tropical Pacific in 2015 are in favor of a scenario in which the thermal signals reflected in the eastern boundaries in late 2014 and early 2015 tended to propagate westward off the equator and then penetrate into the equatorial Pacific in mid-2015. Nevertheless, further detailed studies are critically needed to answer the following important questions. Why can the off-equatorial positive thermal signals be penetrated into the central equatorial region in 2015? What were the driving forces and factors for such a penetration? Why were those potential factors absent in other previous El Niño events, but present in 2015? What were the requirements for such penetrations like in 2015?

These process-oriented analyses provide predictive understanding of the 2015 El Niño event. At present, real-time ENSO predictions exhibit large discrepancies that are strongly model dependent. Various factors affect the real-time prediction, including wind forcing effects (e.g., WWBs and large-scale wind anomalies as a response to SST anomalies) and subsurface thermal effects on SST (as represented by the T_e effect), which are not adequately represented in many current coupled models used for ENSO predictions. For example, preliminary results using the IOCAS ICM indicate that if the positive T_e anomaly effects on SST are underestimated in the SST anomaly equation, then the intensity of the 2015 El Niño event is also underestimated. The relative contributions of wind forcing and subsurface thermal effects to the intensity prediction of the 2015 El Niño event need to be examined using coupled models. Additionally, WWB effects, which are missing in many coupled models used for real-time ENSO predictions, must be adequately represented. Their combined effects with oceanic processes on SST evolution should be examined further to improve the understanding of processes involved in the 2015 El Niño event. More sensitivity experiments along these lines are underway using the IOCAS ICM.

Acknowledgements *We would like to thank Profs. Mu Mu and Dunxin Hu for their comment. The authors wish to thank the two anonymous reviewers for their comments. This research was supported by the National Natural Science Foundation of China (Grant Nos. 41690122, 41690120, 41490644, 41490640 & 41475101), AoShan Talents Program Supported by Qingdao National Laboratory for Marine Science and Technology (Grant No. 2015ASTP), the Chinese Academy of Sciences Strategic Priority Project, the Western Pacific Ocean System (Grant Nos. XDA11010105 & XDA11020306), the National Natural Science Foundation of China-Shandong Joint Fund for Marine Science Research Centers (Grant No. U1406401), and the National Natural Science Foundation of China Innovative Group Grant (Grant No. 41421005), Taishan Scholarship and Qingdao Innovative Program (Grant No. 2014GJJS0101), China Postdoctoral Science Foundation and Qingdao Postdoctoral Application Research Project.*

References

Bjerknes J. 1969. Atmospheric teleconnections from the equatorial pacific. Mon Weather Rev, 97: 163–172

Chen D, Lian T, Fu C, Cane M A, Tang Y, Murtugudde R, Song X, Wu Q, Zhou L. 2015. Strong influence of westerly wind bursts on El Niño diversity. Nat Geosci, 8: 339–345

Gao C, Zhang R H. 2017. The roles of atmospheric wind and entrained water temperature (T_e) in the second-year cooling of the 2010–12 La Niña event. Clim Dyn, 48: 597–617

Hu S, Fedorov A V. 2016. Exceptionally strong easterly wind burst stalling El Niño of 2014. Proc Natl Acad Sci USA, 113: 2005–2010

Jin F F, An S I. 1999. Thermocline and zonal advective feedbacks within the Equatorial ocean recharge oscillator model for ENSO. Geophys Res Lett, 26: 2989–2992

Kalnay E, Kanamitsu M, Kistler R, Collins W, Deaven D, Gandin L, Iredell M, Saha S, White G, Woollen J, Zhu Y, Leetmaa A, Reynolds R, Chelliah M, Ebisuzaki W, Higgins W, Janowiak J, Mo K C, Ropelewski C, Wang J, Jenne R, Joseph D. 1996. The NCEP/NCAR 40-year reanalysis project. Bull Amer Meteorol Soc, 77: 437–471

Keenlyside N, Kleeman R. 2002. Annual cycle of equatorial zonal currents in the Pacific. J Geophys Res, 107: 3093

Levine A F Z, McPhaden M J. 2016. How the July 2014 easterly wind burst gave the 2015-2016 El Niño a head start. Geophys Res Lett, 43: 6503–6510

Liu B Q, Li J Y, Mao J Y, Ren R C, Liu Y M. 2015. Possible mechanism for the development and suspending of El Niño event in 2014 (in Chinese). Chin Sci Bull, 60: 2136

McCreary J P. 1981. A linear stratified ocean model of the equatorial undercurrent. Philos Trans R Soc A-Math Phys Eng Sci, 298: 603–635

McPhaden M J. 2015. Playing hide and seek with El Niño. Nat Clim Change, 5: 791–795

Min Q, Su J, Zhang R, Rong X. 2015. What hindered the El Niño pattern in 2014? Geophys Res Lett, 42: 6762–6770
Reynolds R W, Smith T M. 1994. Improved global sea surface temperature analyses using optimum interpolation. J Clim, 7: 929–948
Zebiak S E, Cane M A. 1987. A model El Ni&ntilde-southern oscillation. Mon Weather Rev, 115: 2262–2278
Zhang C, Li S. 2015. Why is the El Niño event during the 2014 winter not a strong one? (in Chinese). Chin Sci Bull, 60: 1941–1951
Zhang R H, Zebiak S E, Kleeman R, Keenlyside N. 2003. A new intermediate coupled model for El Niño simulation and prediction. Geophys Res Lett, 30: 2012
Zhang R H, Kleeman R, Zebiak S E, Keenlyside N, Raynaud S. 2005. An empirical parameterization of subsurface entrainment temperature for improved SST anomaly simulations in an intermediate ocean model. J Clim, 18: 350–371
Zhang R H, Zheng F, Zhu J, Wang Z. 2013. A successful real-time forecast of the 2010–11 La Niña event. Sci Rep, 3: 1108
Zhang R H, Gao C. 2016a. Role of subsurface entrainment temperature (T_e) in the onset of El Niño events, as represented in an intermediate coupled model. Clim Dyn, 46: 1417–1435
Zhang R H, Gao C. 2016b. The IOCAS intermediate coupled model (IOCAS ICM) and its real-time predictions of the 2015–2016 El Niño event. Sci Bull, 61: 1061–1070
Zhu J, Kumar A, Huang B, Balmaseda M A, Hu Z Z, Marx L, Kinter III J L. 2016. The role of off-equatorial surface temperature anomalies in the 2014 El Niño prediction. Sci Rep, 6: 19677